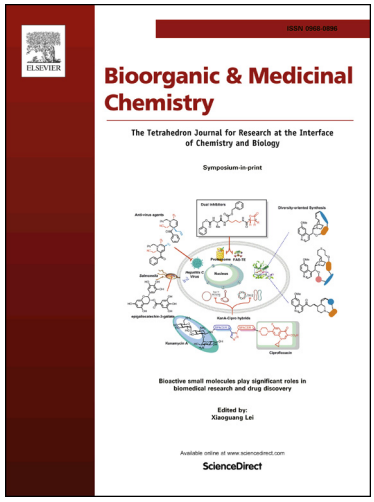

Synthesis and pharmacological evaluation of glycine amide derivatives as novel Vascular Adhesion Protein-1 inhibitors without CYP3A4 and CYP2C19 inhibition

Susumu Yamaki, Yuji Koga, Akira Nagashima, Mitsuhiro Kondo, Yoshiaki Shimada, Keitaro Kadono, Ayako Moritomo, Kosei Yoshihara

PII: S0968-0896(17)30433-9
DOI: http://dx.doi.org/10.1016/j.bmc.2017.05.059
Reference: BMC 13778

To appear in: *Bioorganic & Medicinal Chemistry*

Received Date: 2 March 2017
Revised Date: 8 May 2017
Accepted Date: 30 May 2017

Please cite this article as: Yamaki, S., Koga, Y., Nagashima, A., Kondo, M., Shimada, Y., Kadono, K., Moritomo, A., Yoshihara, K., Synthesis and pharmacological evaluation of glycine amide derivatives as novel Vascular Adhesion Protein-1 inhibitors without CYP3A4 and CYP2C19 inhibition, *Bioorganic & Medicinal Chemistry* (2017), doi: http://dx.doi.org/10.1016/j.bmc.2017.05.059

Synthesis and pharmacological evaluation of glycine amide derivatives as novel Vascular Adhesion Protein-1 inhibitors without CYP3A4 and CYP2C19 inhibition

Susumu Yamaki,* Yuji Koga, Akira Nagashima, Mitsuhiro Kondo, Yoshiaki Shimada, Keitaro Kadono, Ayako Moritomo, and Kosei Yoshihara†

Drug Discovery Research, Astellas Pharma Inc., 21 Miyukigaoka, Tsukuba, Ibaraki 305-8585, Japan

* Corresponding author:

Tel: +81-29-863-6550

Fax: +81-29-852-5387

E-mail: susumu.yamaki@astellas.com

† Present address:

Haupt Pharma Toride Co., Ltd, 5662 Omonmai, Toride, Ibaraki 302-0001, Japan

Abstract

Vascular adhesion protein-1 (VAP-1) is a promising therapeutic target for the treatment of diabetic nephropathy. Here, we conducted optimization studies of our lead compound **1**, which we previously reported as a novel VAP-1 inhibitor, to enhance the inhibition of human VAP-1 and to reduce CYP3A4 and CYP2C19 inhibition. As a result, we identified

3-chloro-4-{4-[5-(3-{[glycyl(methyl)amino]methyl}phenyl)pyrimidin-2-yl]piperazin-1-yl}benzoic acid (**17h**) as a novel orally active VAP-1 inhibitor, with 14-fold increased human VAP-1 inhibitory activity compared to **1**, without CYP3A4 and CYP2C19 inhibition. Oral administration of **17h** significantly inhibited the progression of proteinuria in streptozotocin (STZ) induced diabetic rats at 0.3 and 1 mg/kg, suggesting that this compound has potential to be a therapeutic agent for the treatment of diabetic nephropathy.

Keywords

Vascular adhesion protein-1, Diabetic nephropathy, Glycine amide, CYP2C19, CYP3A4

1. Introduction

Diabetic nephropathy, along with diabetic retinopathy and diabetic neuropathy, is a major diabetic microvascular complication that develops in up to 40% of patients with type 1 and type 2 diabetes.[1] Dialysis is required as symptoms progress, which significantly lowers the quality of life (QOL) of patients. The number of diabetic patients has continued to increase; over 400 million people suffered from diabetes worldwide in 2015, and this number is estimated to increase to more than 600 million by 2040.[2] With the increase in diabetes cases follows an increase in patients with diabetic nephropathy. Furthermore, diabetic nephropathy has become the principal cause of starting dialysis in recent years.[1] Therefore, prevention of the development and progression of diabetic nephropathy is an important issue. The exact cause of diabetic nephropathy is unknown but hyperglycemia and resulting factors, such as acceleration of advanced glycation end-product (AGE) formation, oxidative stress, and (glomerular) hypertension, along with genetic susceptibility are hypothesized to be involved in its development and progression.[3] The current therapeutic strategies for diabetic nephropathy are glycemic control, correction of (glomerular) hypertension, and dietary restriction of protein.[1] Glycemic control has been achieved to some extent by the approval of new drugs with various mechanisms of action, such as dipeptidyl peptidase

4 (DPP4) inhibitors and sodium-glucose cotransporter 2 (SGLT2) inhibitors.[4] Inhibition of the renin-angiotensin system (RAS) also has a beneficial effect on the progression of diabetic nephropathy.[1] However, these current therapeutic strategies are not sufficient as many patients still progress to end-stage renal disease and require dialysis. Therefore, development of novel therapeutic strategies for diabetic nephropathy are needed.

Vascular adhesion protein-1 (VAP-1) was recently reported to be associated with diabetic nephropathy, for example by inducing oxidative stress and accelerating AGE formation.[5] VAP-1 has two known functions:[6] as an adhesion molecule, VAP-1 is involved in leukocyte rolling, adhesion, and transmigration, which are central steps in leukocyte extravasation to sites of inflammation;[7] VAP-1 also acts as an amine oxidase by catalyzing the conversion of biogenic amines into their corresponding aldehydes, while releasing ammonia and hydrogen peroxide.[8] These (cyto)toxic products (aldehydes and hydrogen peroxide) are known to damage the renovasculature directly or indirectly for example by inducing oxidative stress and accelerating AGE formation.[5] Further, increased VAP-1 activity is found in patients with diabetes mellitus, and even higher increases in patients with diabetic microvascular complications such as diabetic retinopathy and diabetic nephropathy.[5] Elevated VAP-1 expression causes increased production of degradated products, such as aldehydes and hydrogen peroxide, and is

therefore considered to contribute to further deterioration of pathologies. These facts suggest that VAP-1 is a promising novel therapeutic target for the treatment of diabetic nephropathy.

Previously, we reported compound **1** (Table 1), a glycine amide derivative, as a novel VAP-1 inhibitor that inhibits rat plasma VAP-1 activity by 60% after oral administration at 1 mg/kg to normal rats.[9] However, this compound inhibited human VAP-1 with less potency than rat VAP-1 (human IC_{50} = 0.34 μM; rat IC_{50} = 0.036 μM). To address this issue, we examined human and rat VAP-1 sequence homology. Taken together with the results of docking analysis of **1** with human VAP-1 model, which we have previously reported,[9] it was found that two amino acid residues (Phe173/Thr, Leu447/Phe) differed around the ligand binding pocket of **1** (Figure 1). Since these two amino acid residues were adjacent to the left phenyl ring of **1**, we hypothesized that species differences in the potency of **1** might be reduced by altering this moiety. We have already reported that introducing a substituent into the 2- or 3-position of the left phenyl ring results in attenuation of VAP-1 inhibitory activity, and that the 4-position is an optimal position for introducing substituent groups.[9] On the other hand, replacement with a hetero aromatic ring has not been attempted; thus, in this study, we converted the left phenyl ring into a hetero aromatic ring.

Besides species differences, **1** also inhibited CYP3A4 and CYP2C19 (Table 1). CYP3A4 and CYP2C19 are members of the CYP450 family and play major roles in drug metabolism; in particular, CYP3A4 is reported to be involved in the metabolism of almost 50% of approved drugs.[10] CYP inhibition may mediate drug-drug interactions (DDIs) that can lead to serious adverse effects or a reduction in drug efficacy. A drug with DDI risk should be carefully prescribed, especially to elderly people who often suffer from multiple diseases and are prescribed multiple drugs. As diabetic nephropathy is prevalent in aged diabetic patients, an agent without CYP inhibition would be optimal for the treatment of diabetic nephropathy. Thus, optimization of compound **1** to reduce inhibitory activity against CYP3A4 and CYP2C19 is required. We focused on reducing CYP3A4 and CYP2C19 inhibition because inhibition of other major isoforms (CYP1A2, CYP2C9, and CYP2D6) was not a concern for compound **1**.

Here, we describe the synthesis of a novel series of glycine amide derivatives, and the successful development of an orally active VAP-1 inhibitor without CYP3A4 and CYP2C19 inhibition.

Table 1

Profile of compound **1**

Structure	VAP-1 IC_{50} (μM)[a]		Rat ex vivo[b]		CYP inhibition (Residual activity)[c]	
	Human	Rat	Dose (mg/kg, po)	Inhibition ratio (at 1 h)	3A4	2C19
	0.34	0.036	1	60%	57%	63%

[a] IC_{50} values are shown as the mean of independent experiments (n = 2).

[b] Inhibitory effect on plasma VAP-1 activity in rats (n = 4) at 1 h after oral administration of compound **1**.

[c] Residual activity of human liver microsomes (HLM) was evaluated using midazolam (for CYP3A4) or *S*-mephenytoin (for CYP2C19) as a probe substrate. Details are described in Section 5.4.

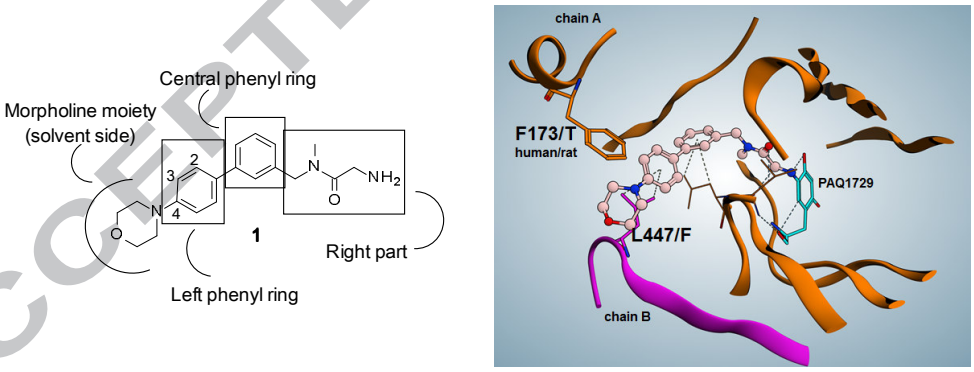

(a) **(b)**

Figure 1. (a) Structure of compound **1**. (b) Molecular modeling results for compound **1** (pale pink, ball and stick) with human VAP-1. Phe173 and Leu447, both depicted as a stick, are the residues that differ between human and rat VAP-1（Thr173 and Phe447, respectively, in rat VAP-1）.

2. Chemistry

The synthesis of glycine amide derivatives is outlined in Schemes 1–3. In Scheme 1, Suzuki-Miyaura coupling between aryl bromide **2**[11] with boronic esters **3a**–**b** followed by removal of *tert*-butoxycarbonyl (Boc) group afforded **5a**–**b**. Miyaura borylation of compound **2** gave boronic ester **6**. Suzuki-Miyaura coupling of **6** with **7** followed by deprotection of Boc group yielded **9**.

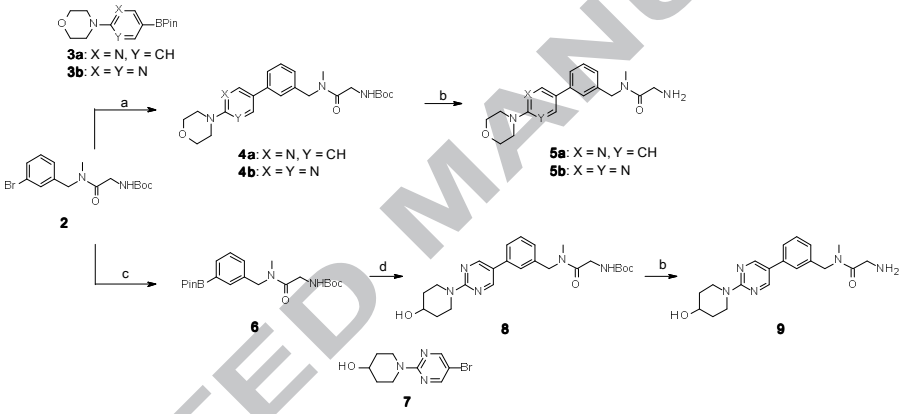

Scheme 1. Reagents and conditions: (a) **3a** or **3b**, $Pd(PPh_3)_4$, Na_2CO_3, DME/H_2O, 90 °C; (b) 4 M HCl (EtOAc solution), MeOH; (c) $B_2(Pin)_2$, $PdCl_2(PPh_3)_2$, KOAc, dioxane, 80 °C; (d) **7**, $Pd(PPh_3)_4$, Na_2CO_3, DME/H_2O, 90 °C.

The synthesis of **14a**–**b** is shown in Scheme 2. Condensation of **10a**–**b** with *N*-Boc-glycine gave **11a**–**b**. Suzuki-Miyaura coupling of **11a**–**b** with **12** followed by deprotection of Boc group yielded **14a**–**b**.

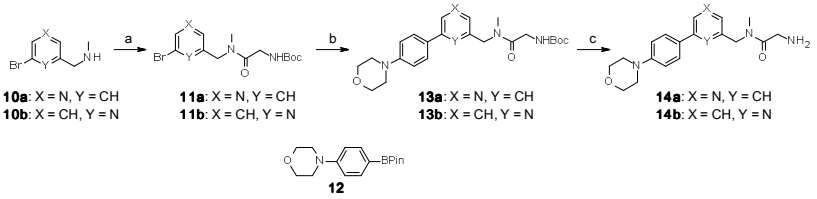

Scheme 2. Reagents and conditions: (a) *N*-Boc-glycine, WSCD·HCl, HOBt, CH_2Cl_2; (b) **12**, $Pd(PPh_3)_4$, Na_2CO_3, DME/H_2O, 80 °C; (c) 4 M HCl (EtOAc solution), EtOAc or MeOH.

Scheme 3 shows the preparation of compounds **17a–h**. Suzuki-Miyaura coupling between boronic ester **6** with 5-bromo-2-chloropyrimidine gave **15**. Substitution of **15** with corresponding amines gave **16a–h**. Deprotection of Boc group of **16a–d** afforded **17a–d**. Hydrolysis of **16e–h** by NaOH and subsequent removal of Boc group yielded carboxylic acid analogs **17e–h**.

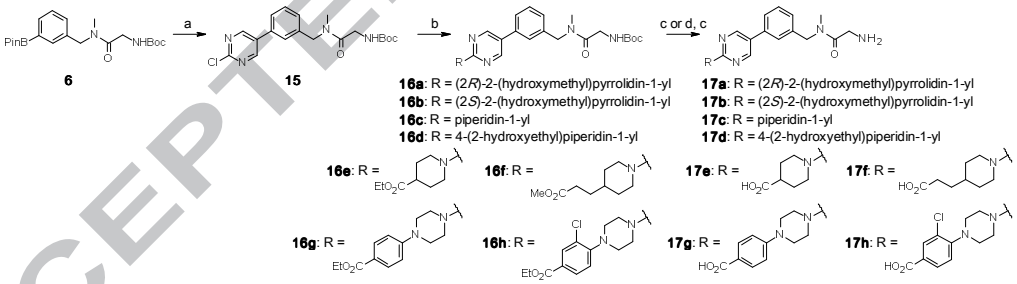

Scheme 3. Reagents and conditions: (a) 5-bromo-2-chloropyrimidine, $Pd(PPh_3)_4$, Na_2CO_3, DME/H_2O, 80 °C; (b) amine, K_2CO_3, DMF, room temperature or 50–60 °C; (c) 4 M HCl (EtOAc or dioxane solution), MeOH or dioxane; (d) 1 M NaOH aq., solvents.

3. Results and discussion

The inhibitory activity of the synthesized compounds against human and rat VAP-1 was measured by a radioenzyme assay using ^{14}C-benzylamine as an artificial substrate. Plasma VAP-1 activity in normal rats after oral administration of test compounds was evaluated using the same radioenzyme assay. Selected compounds were also evaluated for inhibitory activity against CYP3A4 and CYP2C19 using midazolam and *S*-mephenytoin as probe substrates, respectively.

We first examined the effect of converting each phenyl ring of **1** into a pyridine or pyrimidine ring (Table 2). Replacing the left phenyl ring of **1** with a pyridine ring (**5a**) retained rat VAP-1 inhibitory activity (IC_{50} = 0.037 μM). In addition, **5a** showed a 6-fold increase in inhibition of human VAP-1 compared to **1**, with an IC_{50} value of 0.055 μM. The pyrimidine analog **5b** also showed increased VAP-1 inhibitory activity both in rat (2-fold, IC_{50} = 0.015 μM) and in human (11-fold, IC_{50} = 0.031 μM) compared to **1**. These results suggest that the left aryl ring plays an important role in human VAP-1 inhibitory activity, and that its conversion into a hetero aromatic ring reduces the species differences. The enhanced potency of **5b** on human VAP-1 may be explained by electrostatic effects. We calculated the atomic charge distributions of **5b**, **1**, and the electrostatic surface of the ligand binding pocket of human VAP-1 (Figure 2).

For **5b**, negative charge (red) was distributed around the nitrogen atom of the pyrimidine ring (Figure 2a), compared to a positive charge (blue) in the corresponding region in **1** (Figure 2b). In the ligand binding pocket of human VAP-1, a positive charge was distributed around the corresponding site (Figure 2c). While the predicted binding mode of **5b** was similar to that of **1**, **5b** might have higher affinity for human VAP-1 compared to **1** due to these electrostatic effects. This might be responsible for the enhanced potency of **5b** on human VAP-1 compared to that of **1**. As for rat VAP-1, it may have a relatively larger binding pocket around the left phenyl ring of **1** due to a less bulky Thr173 residue compared to the Phe173 in human VAP-1. This larger binding pocket in rat VAP-1 compared to human VAP-1 might have led to reduced electrostatic effects in rat VAP-1, and this led to only a 2-fold increased rat VAP-1 inhibitory activity of **5b** compared to that of **1**.

In contrast, replacing the central phenyl ring of **1** with a pyridine ring (**14a**, **14b**) resulted in reduced inhibition of both human and rat VAP-1. These results suggest that conversion of the central phenyl ring into a pyridine ring is not well tolerated.

Table 2

In vitro activity of biaryl derivatives

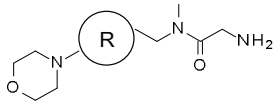

Compound	R	VAP-1 IC_{50} (μM)[a]	
		Human	Rat
1[b]	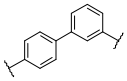	0.34	0.036
5a[c]	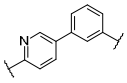	0.055	0.037
5b[c]	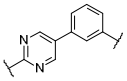	0.031	0.015
14a[c]	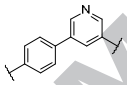	1.5	0.12
14b[d]	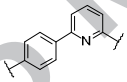	2.0	0.16

[a] IC_{50} value is shown as the mean of independent experiments ($n = 2$).

[b] Ethanedioate salt.

[c] (2*R*, 3*R*)-tartrate salt.

[d] Dihydrochloride salt.

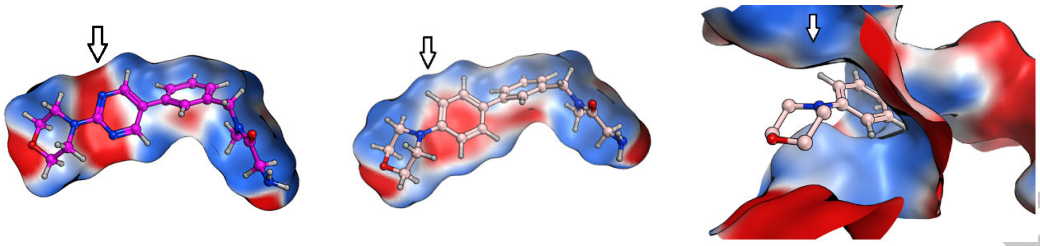

(a) **(b)** **(c)**

Figure 2. Atomic charge distributions of compound **5b** (a), compound **1** (b), and the electrostatic surface of the ligand binding pocket of human VAP-1 (c; the docked compound is **1**). Connolly surfaces[12] are colored red for negative charge and blue for positive charge.

Since **5b** showed improved inhibition of human VAP-1 and reduced species differences, we evaluated its CYP inhibition profile (Table 3). **5b** exhibited reduced inhibition of both CYP3A4 and CYP2C19 (residual activity: 91% and 74%, respectively) compared to **1**. Lowering lipophilicity is known to reduce CYP inhibition,[10,13] which may explain the case here (**1**: CLog*P* = 1.22; **5b**: CLog*P* = 0.59; calculated using ACD Log*P* prediction software[14]). However, as **5b** still inhibited CYP2C19, we considered that there was room for further improvement. Thus, we conducted further optimization of **5b** to reduce its inhibition of CYP2C19 while maintaining VAP-1 inhibitory activity.

Inhibition of CYP2C19 activity can be reduced by introducing polar substituent groups.[10,15] For **5b**, we hypothesized that the optimal position for introducing polar substituent groups is around the morpholine moiety, since this side is predicted to be on the solvent side (Figure 1), and is well tolerated for introduction of additional substituents as we reported previously.[9] In contrast, it would be difficult to introduce polar substituents into the central phenyl ring and the right part (Figure 1) as steric tolerance around these sites are limited.[9] Therefore, we next investigated the introduction of polar substituent groups around the morpholine moiety (Table 4).

Table 3

Profiles of **1** and **5b**

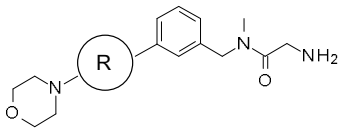

Compound	R	VAP-1 IC_{50} (μM)[a]		CYP inhibition (Residual activity)[b]		CLog*P*[c]
		Human	Rat	3A4	2C19	
1[d]	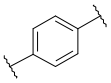	0.34	0.036	57%	63%	1.22
5b[e]	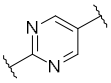	0.031	0.015	91%	74%	0.59

[a] IC_{50} values are shown as the mean of independent experiments ($n = 2$).

[b] Residual activities of HLM were evaluated using midazolam (for CYP3A4) or *S*-mephenytoin (for CYP2C19) as a probe substrate. Details are described in Section 5.4.

[c] CLog*P* values calculated using ACD Log*P* prediction software.[14]

[d] Ethanedioate salt.

[e] (2*R*, 3*R*)-tartrate salt.

To evaluate the effect of introducing polar substituents, we first synthesized an unsubstituted piperidine analog (**17c**), which inhibited human VAP-1 with an IC_{50} value of 0.25 μM. Next, conversion of the morpholinyl group of **5b** into a 2-hydroxymethyl-pyrrolidinyl group (**17a**, **17b**) or 4-hydroxy-piperidinyl group (**9**) resulted in 4–10-fold less potent inhibition of human VAP-1 compared to **5b**. In contrast, the 4-(2-hydroxyethyl)-piperidine derivative **17d** showed equipotent activity (IC_{50} = 0.045 μM) with **5b**. Compared to **17c**, **9** and **17d** exhibited enhanced human VAP-1 inhibitory activities, suggesting that introduction of a hydroxyl group may increase human VAP-1 inhibitory activity and that the position of the hydroxyl group may play an important role in affective inhibition of human VAP-1. Introducing a carboxyl group produced similar observations. While the isonipecotic acid analog **17e** showed approximately 55-fold decreased human VAP-1 inhibitory activity, the 3-(piperidin-4-yl)propanoic acid analog **17f** exhibited only 5-fold less potent activity (IC_{50} = 0.14 μM), compared to **5b**. These results suggest that the position of the carboxyl group also plays an important role in human VAP-1 inhibitory activity. Regarding CYP inhibition, while **17d** showed slightly reduced inhibition of CYP2C19 (residual activity: 82%), it inhibited CYP3A4 (residual activity: 46%). In contrast, the introduction of carboxyl group (**17e**, **17f**) abolished inhibition of both CYP2C19 and

CYP3A4. These results suggest that introduction of a carboxyl group is effective in reducing CYP inhibition. Accordingly, we focused on optimization of carboxylic acid derivatives to enhance VAP-1 inhibitory activity while maintaining reduced CYP inhibition. Since the position of the carboxyl group was important for inhibiting human VAP-1 (**17e** versus **17f**), we hypothesized that fixing the carboxyl group at a more optimal position than that in **17f** may improve VAP-1 inhibition. Based on this speculation, we evaluated a benzoic acid analog, which has a more rigid structure than **17f**. For convenience of synthesis, a piperazine type was synthesized. Fortunately, the benzoic acid analog **17g** exhibited more than 6-fold potent human VAP-1 inhibitory activity compared to **17f**. According to structure-activity relationship (SAR) studies of structurally related compounds, introduction of a substituent at the 2-position of the phenyl group at the left end is well tolerated (data not shown); thus, we evaluated a 2-substitued benzoic acid analog. The 2-chloro derivative **17h** showed equipotent inhibition of human VAP-1 with **17g**. Further, **17g** and **17h** both exhibited reduced CYP inhibition, as expected.

Table 4

Substituent effect on VAP-1 potency and CYP inhibition.

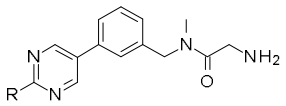

Compound	R	Human VAP-1 IC_{50} (μM)[a]	CYP inhibition (Residual activity)[b]	
			3A4	2C19
5b[c]		0.031	91%	74%
17c[d]		0.25	NT[e]	NT[e]
17a[d]	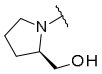	0.30	NT[e]	NT[e]
17b[d]	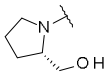	0.24	NT[e]	NT[e]
9[c]	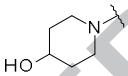	0.13	NT[e]	NT[e]
17d[c]	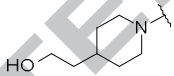	0.045	46%	82%
17e[d]	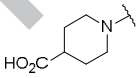	1.7	112%	104%
17f[d]	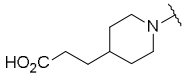	0.14	108%	119%
17g[d]	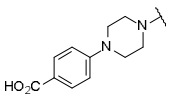	0.024	100%	106%
17h[d]	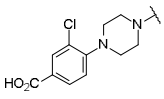	0.025	98%	109%

[a] IC_{50} values are shown as the mean of independent experiments ($n = 2$).

[b] Residual activities of HLM were evaluated using midazolam (for CYP3A4) or *S*-mephenytoin (for CYP2C19) as a probe substrate. Details are described in Section 5.4.

[c] (2*R*, 3*R*)-tartrate salt.
[d] Dihydrochloride salt.
[e] NT = not tested.

To elucidate the mechanisms governing the improved potency of benzoic acid derivatives like **17g** and **17h** to inhibit human VAP-1, we conducted docking analysis of **17h** with human VAP-1 (Figure 3). This model revealed several interactions. First, **17h** formed three CH-π interactions with human VAP-1: central phenyl ring with Leu469, pyrimidine ring[16] with Leu447, and the hydrogen in the piperazine with Tyr394. Second, **17h** formed two CH-O interactions with human VAP-1: the oxygen in the glycine amide moiety[17] with Leu468, and the hydrogen at the α-position of the carbonyl group in the glycine amide moiety with the carbonyl oxygen of the Leu468 backbone. Third, the chloro group formed a halogen-O interaction with the carbonyl oxygen of the ASP446 backbone. In addition to these interactions, increased Van der Waals interaction due to higher molecular weight compared to **1**, and the electrostatic effects of the pyrimidine ring described above may also contribute to potent VAP-1 inhibitory activity of **17h**. The enhancement of in vitro potency by the introduction of a carboxyl group (**17c** versus **17f**, **17g**, and **17h**) might be explained by the presence of basic residues like His450 and Lys423 around this functional group. Although the effect of the phenyl group on the left end and the nitrogen atom in the piperazine ring is not clear,

one of the reasons for the improved potency of benzoic acid derivatives like **17g** and **17h** compared to the 3-(piperidin-4-yl)propanoic acid analog **17f** may be due to the fixed optimal position of the carboxyl group of benzoic acid derivatives with respect to these basic resides.

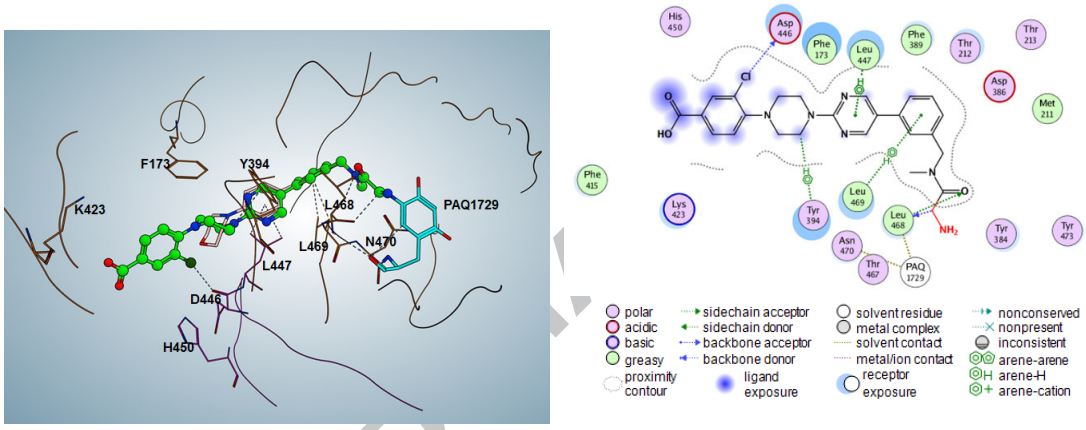

(a) **(b)**

Figure 3. (a) Molecular modeling results for **1** (pale pink) and **17h** (green, ball and stick) with human VAP-1. (b) Two-dimensional diagram prepared by the ligand interactions application in MOE[18b]. Arrows indicate interactions.

Based on their enhanced human VAP-1 inhibitory activity without CYP3A4 and CYP2C19 inhibition, **17g** and **17h** were selected for further evaluation (Table 5). As for in vitro potency against rat VAP-1, **17g** and **17h** showed comparable activities to that of human VAP-1 with IC_{50} values of 0.010 μM and 0.015 μM, respectively, resulting in reduced species differences compared to **1** (**1**: human IC_{50} = 0.34 μM; rat IC_{50} = 0.036 μM). Encouraged by this result, we next evaluated the ex vivo efficacy of these compounds. Oral administration of **17g** and **17h** at 1 mg/kg inhibited rat plasma VAP-1 activity by 68% and 96% (after 1 h), respectively. Furthermore, **17h** inhibited VAP-1 in rat plasma at lower doses, with oral administration at 0.3 mg/kg resulting in 64% inhibition of rat plasma VAP-1. The inhibitory effects of these compounds on plasma VAP-1 activity were similar at 1 and 6 h after oral administration. The more potent ex vivo efficacy of **17h** compared to **17g** may be explained in part by the improved aqueous solubility of **17h**, especially in the presence of sodium taurocholate, compared to **17g**, since compounds with low aqueous solubility are more likely to have poor bioavailability.[19] The improved aqueous solubility of **17h** might be due to disruption of the molecular symmetry by introduction of a chloro group at the ortho position.[20]

The pharmacokinetic profile of **17h** is shown in Table 6. Although the bioavailability of **17h** was only 17%, oral administration at 1 mg/kg resulted in a plasma concentration

of 111 ng/mL after 1 h, which is approximately 15 times higher than its IC_{50} value (0.015 μM, rat). Therefore, the ex vivo efficacy of **17h** at 1 h was considered reasonable. Further, while the plasma concentration of **17h** at 6 h post administration (7.1 ng/mL) was just below the IC_{50} value, its inhibitory effect on plasma VAP-1 activity was similar to that observed after 1 h (1 h: 96% inhibition; 6 h: 93% inhibition). Therefore, we speculated that once **17h** forms a Schiff base intermediate with topaquinone (TPQ) in the active site of VAP-1, its dissociation may be slowed such as to prolong the duration of its ex vivo efficacy despite a decrease in plasma concentration.

Table 5

Profiles of **17g** and **17h**

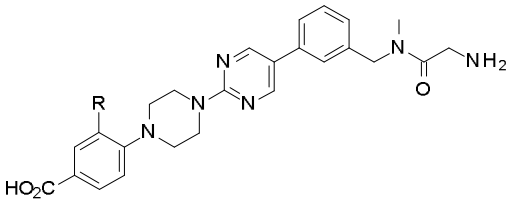

Compound	R	VAP-1 IC_{50} (μM)[a]		CYP inhibition (Residual activity)[b]		Rat ex vivo[c]			Solubility (μM)[d]	
		Human	Rat	3A4	2C19	Dose (mg/kg, po)	Inhibition ratio at 1 h	Inhibition ratio at 6 h	JP2	JP2 + TC
17g[e]	H	0.024	0.010	100%	106%	1	68%	60%	<1	<1
17h[e]	Cl	0.025	0.015	98%	109%	1	96%	93%	2.3	89.6
						0.3	64%	62%		

[a] IC_{50} values are shown as the mean of independent experiments ($n = 2$).

[b] Residual activities of HLM were evaluated using midazolam (for CYP3A4) or *S*-mephenytoin (for CYP2C19) as a probe substrate. Details are described in Section 5.4.

[c] Inhibitory effect on plasma VAP-1 activity in rats ($n = 4$) at 1 h or 6 h after oral administration of test compounds.

[d] Aqueous solubility in 2nd fluid for disintegration test in Japanese Pharmacopeia (JP2; pH = 6.8) or in JP2 + 15 mM of sodium taurocholate (JP2 + TC).

[e] Dihydrochloride salt.

Table 6

Pharmacokinetic profiles of compound **17h** in rats

Route	$AUC_{0\text{-}24h}$ (ng·h/mL)	C_{max} (ng/mL)	CL_{tot} (mL/min/kg)	$t_{1/2}$ (h)	V_{dss} (L/kg)	BA (%)
iv (1 mg/kg)	1920		8.69	1.39	0.386	
po (1 mg/kg)	334	113		1.29		17.4

Encouraged by these results, we next investigated the in vivo efficacy of **17h** on the progression of proteinuria in STZ-induced diabetic rats. As shown in Figure 4, oral administration of **17h** at 0.3 and 1 mg/kg significantly inhibited progression of proteinuria. **17h** also significantly inhibited plasma VAP-1 activity in STZ-induced rats after 4 weeks of administration at 0.3 and 1 mg/kg. These results suggest that progression of proteinuria in STZ-induced rats is suppressed by inhibition of VAP-1, and that **17h** may have a beneficial effect for the treatment of diabetic nephropathy.

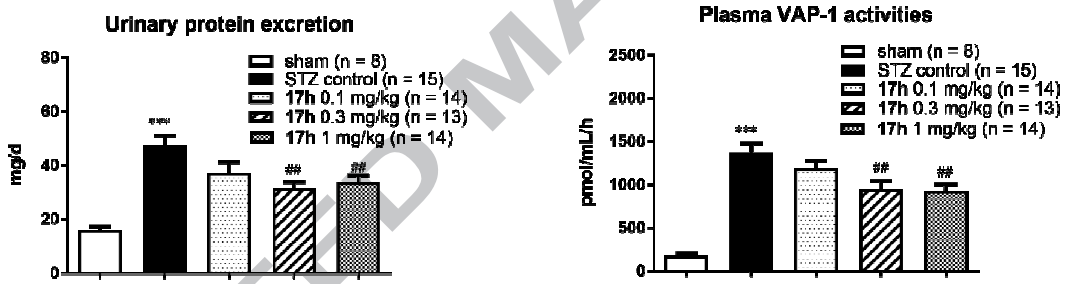

(a) **(b)**

Figure 4. (a) Effect of oral administration of **17h** on the progression of proteinuria in STZ-induced diabetic rats. (b) Inhibitory effect on plasma VAP-1 activity 24 h after the final dose of a 4-week **17h** regimen in STZ-induced diabetic rats. The data represent the mean ± SEM: ***p<0.001 versus sham group (Student's t-test), $^{\#\#}p$<0.01 versus STZ control group (Dunnett's multiple comparison test).

4. Conclusion

In this study, we conducted structural optimization of our lead compound **1** to identify a novel orally active VAP-1 inhibitor for the treatment of diabetic nephropathy. Based on molecular modeling analysis and protein sequence information, we found that replacement of the left phenyl ring in **1** with a pyrimidine ring lead to over 10-fold greater inhibition of human VAP-1 compared to **1**. Further, reduced inhibition of CYP3A4 and CYP2C19 while maintaining VAP-1 inhibitory activity was achieved by the introduction of a carboxyl group at the appropriate position. These findings led to the identification of benzoic acid analogs like **17g** and **17h**, which had enhanced human VAP-1 inhibitory activity without CYP3A4 and CYP2C19 inhibition. Of these compounds, **17h** showed more potent ex vivo efficacy, with rat plasma VAP-1 inhibitory activity of 64% at 1 h after oral administration at 0.3 mg/kg. Oral administration of **17h** at 0.3 and 1 mg/kg significantly inhibited the progression of proteinuria in STZ-induced diabetic rats, suggesting that this compound may have a beneficial effect for the treatment of diabetic nephropathy.

5. Experimental

5.1 Chemistry

^{1}H NMR spectra were recorded on a Varian VNS-400, JEOL JNM-LA400 or JEOL JNM-AL400 spectrometer. Chemical shifts were expressed in δ values (ppm) using tetramethylsilane as the internal standard (s = singlet, d = doublet, t = triplet, q = quartet, m = multiplet, dd = double doublet, dt = double triplet, and br = broad peak). Mass spectra (MS) were recorded on a JEOL LX-2000, Waters ZQ-2000, Waters LCT Premier mass spectrometer or Thermo Fisher Exactive Plus Orbitrap. Elemental analyses were conducted using a Yanaco JM10 (C, H, N), Elementar Vario EL III (C, H, N), Dionex ICS-3000 (S, halogen), and Dionex DX-5000 (S, halogen) and were within ±0.4% of theoretical values. All reactions were carried out using commercially available reagents and solvents without further purification. The following abbreviations are used: Ar, aryl; $CHCl_3$, chloroform; CH_2Cl_2, dichloromethane; *i*Pr_2O, diisopropyl ether; DME, 1,2-dimethoxyethane; DMF, *N*,*N*-dimethylformamide; DMSO, dimethyl sulfoxide; EtOAc, ethyl acetate; EtOH, ethanol; WSCD, 1-ethyl-3-(3'-dimethylaminopropyl) carbodiimide HCl, hydrochloric acid; HOBt, 1-hydroxybenzotriazole; $MgSO_4$, magnesium sulfate; MeOH, methanol; KOAc, potassium acetate; K_2CO_3, potassium carbonate; Na_2CO_3, sodium carbonate; $NaHCO_3$, sodium hydrogen carbonate; NaOH,

sodium hydroxide; Na_2SO_4, sodium sulfate; and THF, tetrahydrofuran.

5.1.1. *tert*-Butyl [2-(methyl{3-[6-(morpholin-4-yl)pyridin-3-yl]benzyl}amino)-2-oxoethyl]carbamate (4a)

To a mixture of *tert*-butyl {2-[(3-bromobenzyl)(methyl)amino]-2-oxoethyl}carbamate (**2**; 226 mg, 0.63 mmol) in DME (2.3 mL)/water (1.1 mL) were added 4-[5-(4,4,5,5-tetramethyl-1,3,2-dioxaborolan-2-yl)pyridin-2-yl]morpholine (**3a**; 193 mg, 0.66 mmol), Na_2CO_3 (201 mg, 1.90 mmol), and $Pd(PPh_3)_4$ (22 mg, 0.019 mmol) under a nitrogen atmosphere. The mixture was stirred at 90 °C for 24 h. After being cooled to room temperature, the mixture was concentrated in vacuo. The residue was diluted with water and extracted with $CHCl_3$. The organic layer was dried over $MgSO_4$ and concentrated in vacuo. The residue was purified by column chromatography on silica gel ($CHCl_3$/MeOH = 98:2), and washed with iPr$_2$O to give the product (230 mg, 83%) as a colorless solid. ^{1}H NMR ($CDCl_3$): this compound exists as a pair of rotamers at room temperature. δ 1.44 (minor rotamer, 9H, s), 1.46 (major rotamer, 9H, s), 2.92 (major rotamer, 3H, s), 3.02 (minor rotamer, 3H, s), 3.51–3.64 (4H, m), 3.81–3.93 (4H, m), 4.02 (major rotamer, 2H, d, J = 3.9 Hz), 4.06 (minor rotamer, 2H, d, J = 3.9 Hz),

4.52 (minor rotamer, 2H, s), 4.66 (major rotamer, 2H, s), 5.57 (1H, brs), 6.72 (1H, d, J = 8.7 Hz), 7.07–7.81 (5H, m), 8.43 (1H, s); MS (ESI) m/z $[M+H]^+$ 441.

5.1.2. *tert*-Butyl [2-(methyl{3-[2-(morpholin-4-yl)pyrimidin-5-yl]benzyl}amino)-2-oxoethyl]carbamate (4b)

Compound **4b** was prepared from **2** and 4-[5-(4,4,5,5-tetramethyl-1,3,2-dioxaborolan-2-yl)pyrimidin-2-yl]morpholine (**3b**) in 94% yield as a colorless oil, using a similar approach to that described for **4a**. ^{1}H NMR ($CDCl_3$): this compound exists as a pair of rotamers at room temperature. δ 1.44 (minor rotamer, 9H, s), 1.46 (major rotamer, 9H, s), 2.92 (major rotamer, 3H, s), 3.02 (minor rotamer, 3H, s), 3.71–3.93 (8H, m), 3.97–4.10 (2H, m), 4.53 (minor rotamer, 2H, s), 4.66 (major rotamer, 2H, s), 5.56 (1H, brs), 7.09–7.74 (4H, m), 8.55 (major rotamer, 2H, s), 8.56 (minor rotamer, 2H, s); MS (ESI) m/z $[M+H]^+$ 442.

5.1.3. *N*-Methyl-*N*-{3-[6-(morpholin-4-yl)pyridin-3-yl]benzyl}glycinamide (2*R*, 3*R*)-tartrate (5a)

To a solution of **4a** (220 mg, 0.50 mmol) in MeOH was added 4 M HCl/EtOAc (1.25 mL, 5.00 mmol). After being stirred at room temperature for 4 h, the mixture was concentrated in vacuo. The residue was diluted with saturated $NaHCO_3$ aqueous

solution, and the mixture was extracted with $CHCl_3$. The organic layer was dried over $MgSO_4$ and concentrated in vacuo. To a solution of the residue in EtOH was added (2*R*, 3*R*)-tartaric acid (75 mg, 0.50 mmol). The resulting precipitate was filtered to give the product (135 mg, 55%) as a colorless solid. ^{1}H NMR (DMSO-d_6): this compound exists as a pair of rotamers at room temperature. δ 2.90 (minor rotamer, 3H, s), 2.96 (major rotamer, 3H, s), 3.46–3.54 (4H, m), 3.68–3.76 (4H, m), 3.93 (minor rotamer, 2H, s), 3.98 (major rotamer, 2H, s), 4.15 (2H, s, tartaric acid), 4.59 (minor rotamer, 2H, s), 4.62 (major rotamer, 2H, s), 6.93 (major rotamer, 1H, d, J = 8.9 Hz), 6.94 (minor rotamer, 1H, d, J = 8.9 Hz), 7.16–7.23 (1H, m), 7.37–7.50 (2H, m), 7.51–7.56 (major rotamer, 1H, m), 7.56–7.61 (minor rotamer, 1H, m), 7.84–7.92 (1H, m), 8.47 (major rotamer, 1H, d, J = 2.5 Hz), 8.49 (minor rotamer, 1H, d, J = 2.4 Hz); MS (ESI) *m/z* $[M+H]^+$ 341; HRMS (ESI) *m/z* Calcted for $C_{19}H_{25}N_4O_2$ $[M+H]^+$: 341.1972, Found: 341.1975.

5.1.4. *N*-Methyl-*N*-{3-[2-(morpholin-4-yl)pyrimidin-5-yl]benzyl}glycinamide (2*R*, 3*R*)-tartrate (5b)

Compound **5b** was prepared from **4b** in 75% yield as a colorless solid, using a similar approach to that described for **5a**. ^{1}H NMR (DMSO-d_6): this compound exists as a pair of rotamers at room temperature. δ 2.88 (minor rotamer, 3H, s), 2.93 (major rotamer, 3H, s), 3.64–3.80 (12H, m), 4.56 (minor rotamer, 2H, s), 4.60 (major rotamer, 2H, s),

7.17–7.24 (1H, m), 7.39–7.50 (2H, m), 7.52–7.57 (major rotamer, 1H, m), 7.57–7.62 (minor rotamer, 1H, m), 8.72 (major rotamer, 2H, s), 8.74 (minor rotamer, 2H, s); MS (ESI) *m/z* $[M+H]^+$ 342; HRMS (ESI) *m/z* Calcted for $C_{18}H_{24}N_5O_2$ $[M+H]^+$: 342.1925, Found: 342.1927.

5.1.5. *tert*-Butyl (2-{methyl[3-(4,4,5,5-tetramethyl-1,3,2-dioxaborolan-2-yl)benzyl]amino}-2-oxoethyl)carbamate (6)

To a mixture of **2** (31.3 g, 87.7 mmol) in dioxane (319 mL) were added 4,4,4',4',5,5,5',5'-octamethyl-2,2'-bi-1,3,2-dioxaborolane (24.5 g, 96.4 mmol), KOAc (25.8 g, 263 mmol), and $PdCl_2(PPh_3)_2$ (2.91 g, 4.15 mmol) under an argon atmosphere. The mixture was stirred at 80 °C for 18 h. After being cooled to room temperature, the mixture was concentrated in vacuo. The residue was diluted with water and extracted with $CHCl_3$. The organic layer was dried over Na_2SO_4 and concentrated in vacuo. The residue was purified by column chromatography on silica gel (hexane/EtOAc = 5:1 to 1:1) to afford a solid. This solid was suspended in iPr_2O, and the mixture was stirred at room temperature, added hexane, and stirred under ice-cooling. The resulting precipitate was filtered to give the product (29.4 g, 83%) as a solid. ^1H NMR ($CDCl_3$): this compound exists as a pair of rotamers at room temperature. δ 1.35 (major rotamer, 12H,

s), 1.35 (minor rotamer, 12H, s), 1.44 (minor rotamer, 9H, s), 1.46 (major rotamer, 9H, s), 2.86 (major rotamer, 3H, s), 2.96 (minor rotamer, 3H, s), 4.01 (major rotamer, 2H, d, J = 4.2 Hz), 4.05 (minor rotamer, 2H, d, J = 4.2 Hz), 4.46 (minor rotamer, 2H, s), 4.62 (major rotamer, 2H, s), 5.51–5.64 (1H, brm), 7.21–7.40 (2H, m), 7.59 (minor rotamer, 1H, s), 7.64 (major rotamer, 1H, s), 7.71–7.77 (1H, m); MS (ESI) *m/z* $[M+H]^+$ 405.

5.1.6. *tert*-Butyl {2-[{3-[2-(4-hydroxypiperidin-1-yl)pyrimidin-5-yl]benzyl}(methyl)amino]-2-oxoethyl}carbamate (8)

Compound **8** was prepared from **6** and 1-(5-bromopyrimidin-2-yl)piperidin-4-ol (**7**) in 94% yield as a pale yellow oil, using a similar approach to that described for **4a**. ^{1}H NMR ($CDCl_3$): this compound exists as a pair of rotamers at room temperature. δ 1.44 (minor rotamer, 9H, s), 1.46 (major rotamer, 9H, s), 1.41–1.68 (2H, m), 1.91–2.07 (2H, m), 2.92 (major rotamer, 3H, s), 3.01 (minor rotamer, 3H, s), 3.29–3.48 (2H, m), 3.90–4.10 (3H, m), 4.36–4.56 (2H, m), 4.52 (minor rotamer, 2H, s), 4.65 (major rotamer, 2H, s), 5.57 (1H, brs), 7.04–7.48 (4H, m), 8.53 (2H, s); MS (ESI) *m/z* $[M+H]^+$ 456.

5.1.7. *N*-{3-[2-(4-Hydroxypiperidin-1-yl)pyrimidin-5-yl]benzyl}-*N*-methylglycinamide (2*R*, 3*R*)-tartrate (9)

Compound **9** was prepared from **8** in 48% yield as a colorless solid, using a similar approach to that described for **5a**. ^{1}H NMR (DMSO-d_6): this compound exists as a pair of rotamers at room temperature. δ 1.27–1.41 (2H, m), 1.73–1.85 (2H, m), 2.90 (minor rotamer, 3H, s), 2.96 (major rotamer, 3H, s), 3.27–3.38 (2H, m), 3.72–3.81 (1H, m), 3.93 (minor rotamer, 2H, s), 3.99 (major rotamer, 2H, s), 4.17 (2H, s, tartaric acid), 4.25–4.35 (2H, m), 4.58 (minor rotamer, 2H, s), 4.62 (major rotamer, 2H, s), 7.18–7.25 (1H, m), 7.39–7.50 (2H, m), 7.52–7.57 (major rotamer, 1H, m), 7.57–7.62 (minor rotamer, 1H, m), 8.67 (major rotamer, 2H, s), 8.70 (minor rotamer, 2H, s); MS (FAB) *m/z* $[M+H]^+$ 356.

5.1.8. *tert*-Butyl (2-{[(5-bromopyridin-3-yl)methyl](methyl)amino}-2-oxoethyl)carbamate (11a)

To a solution of 1-(5-bromopyridin-3-yl)-*N*-methylmethanamine (**10a**; 1.37 g, 6.81 mmol) in CH_2Cl_2 (20 mL) were added *N*-(*tert*-butoxycarbonyl)glycine (1.37 g, 7.83 mmol), WSCD·HCl (1.72 g, 8.95 mmol), and HOBt (1.20 g, 8.89 mmol). After being stirred at room temperature overnight, the mixture was diluted with saturated $NaHCO_3$ aqueous solution and extracted with $CHCl_3$. The organic layer was dried over Na_2SO_4, and concentrated in vacuo. The residue was purified by column chromatography on silica gel (hexane/EtOAc = 4:1 to 1:2) to give the product (2.02 g, 83%). ^{1}H NMR ($CDCl_3$): this compound exists as a pair of rotamers at room temperature. δ 1.36 (minor rotamer, 9H, s), 1.39 (major rotamer, 9H, s), 2.79 (minor rotamer, 3H, s), 2.96 (major

rotamer, 3H, s), 3.79–3.88 (2H, m), 4.53 (major rotamer, 2H, s), 4.60 (minor rotamer, 2H, s), 6.76–6.85 (major rotamer, 1H, m), 6.85–6.91 (minor rotamer, 1H, m), 7.86–7.91 (major rotamer, 1H, m), 7.93–7.97 (minor rotamer, 1H, m), 8.43–8.49 (1H, m), 8.61 (major rotamer, 1H, d, J = 2.1 Hz), 8.66 (minor rotamer, 1H, d, J = 2.0 Hz); MS (FAB) m/z $[M+H]^+$ 358.

5.1.9. *tert*-Butyl (2-{[(6-bromopyridin-2-yl)methyl](methyl)amino}-2-oxoethyl)carbamate (11b)

Compound **11b** was prepared from **10b** in 54% yield, using a similar approach to that described for **11a**. ^{1}H NMR ($CDCl_3$): this compound exists as a pair of rotamers at room temperature. δ 1.44 (minor rotamer, 9H, s), 1.46 (major rotamer, 9H, s), 3.03 (minor rotamer, 3H, s), 3.05 (major rotamer, 3H, s), 3.99–4.07 (2H, m), 4.53 (minor rotamer, 2H, s), 4.68 (major rotamer, 2H, s), 5.48 (1H, brs), 7.10 (minor rotamer, 1H, d, J = 7.4 Hz), 7.20 (major rotamer, 1H, d, J = 7.5 Hz), 7.39 (major rotamer, 1H, d, J = 7.7 Hz), 7.43 (minor rotamer, 1H, d, J = 7.8 Hz), 7.51 (major rotamer, 1H, dd, J = 7.8, 7.8 Hz), 7.56 (minor rotamer, 1H, dd, J = 7.7, 7.7 Hz); MS (FAB) m/z $[M+H]^+$ 358.

5.1.10. *tert*-Butyl {2-[methyl({5-[4-(morpholin-4-yl)phenyl]pyridin-3-yl}methyl)amino]-2-oxoethyl}carbamate (13a)

Compound **13a** was prepared from **11a** and 4-[4-(4,4,5,5-tetramethyl-1,3,2-dioxaborolan-2-yl)phenyl]morpholine (**12**) in 75% yield, using a similar approach to that described for **4a**. ^{1}H NMR (DMSO-d_6): this compound exists as a pair of rotamers at room temperature. δ 1.37 (minor rotamer, 9H, s), 1.39 (major rotamer, 9H, s), 2.82 (minor rotamer, 3H, s), 2.97 (major rotamer, 3H, s), 3.13–3.20 (4H, m), 3.73–3.79 (4H, m), 3.85 (major rotamer, 2H, d, J = 5.9 Hz), 3.89 (minor rotamer, 2H, d, J = 6.0 Hz), 4.58 (major rotamer, 2H, s), 4.64 (minor rotamer, 2H, s), 6.82 (major rotamer, 1H, t, J = 5.8 Hz), 6.94 (minor rotamer, 1H, t, J = 5.9 Hz), 7.05 (2H, d, J = 8.8 Hz), 7.61 (major rotamer, 2H, d, J = 8.7 Hz), 7.68 (minor rotamer, 2H, d, J = 8.7 Hz), 7.80–7.84 (major rotamer, 1H, m), 7.86–7.90 (minor rotamer, 1H, m), 8.33–8.40 (1H, m), 8.72–8.76 (major rotamer, 1H, m), 8.77–8.81 (minor rotamer, 1H, m); MS (ESI) *m/z* $[M+H]^+$ 441.

5.1.11. *tert*-Butyl {2-[methyl({6-[4-(morpholin-4-yl)phenyl]pyridin-2-yl}methyl)amino]-2-oxoethyl}carbamate (13b)

Compound **13b** was prepared from **11b** and 4-[4-(4,4,5,5-tetramethyl-1,3,2-dioxaborolan-2-yl)phenyl]morpholine (**12**) in 69% yield, using a similar approach to that described for **4a**. ^{1}H NMR (DMSO-d_6): this compound

exists as a pair of rotamers at room temperature. δ 1.37 (minor rotamer, 9H, s), 1.39 (major rotamer, 9H, s), 2.88 (minor rotamer, 3H, s), 3.07 (major rotamer, 3H, s), 3.16–3.22 (4H, m), 3.72–3.79 (4H, m), 3.90 (major rotamer, 2H, d, J = 5.7 Hz), 3.98 (minor rotamer, 2H, d, J = 5.8 Hz), 4.62 (major rotamer, 2H, s), 4.63 (minor rotamer, 2H, s), 6.73–6.81 (1H, m), 6.98–7.17 (3H, m), 7.70–7.85 (2H, m), 7.94–8.02 (2H, m); MS (FAB) *m/z* $[M+H]^+$ 441.

5.1.12.

***N*-Methyl-*N*-({5-[4-(morpholin-4-yl)phenyl]pyridin-3-yl}methyl)glycinamide (2*R*, 3*R*)-tartrate (14a)**

Compound **14a** was prepared from **13a** in 75% yield as a colorless solid, using a similar approach to that described for **5a**. ^{1}H NMR (DMSO-d_6): this compound exists as a pair of rotamers at room temperature. δ 2.89 (minor rotamer, 3H, s), 2.99 (major rotamer, 3H, s), 3.13–3.22 (4H, m), 3.72–3.79 (4H, m), 3.83 (2H, s, tartaric acid), 3.91 (major rotamer, 2H, s), 3.92 (minor rotamer, 2H, s), 4.62 (minor rotamer, 2H, s), 4.64 (major rotamer, 2H, s), 7.01–7.11 (2H, m), 7.56–7.67 (2H, m), 7.82–7.88 (1H, m), 8.41 (1H, d, J = 1.7 Hz), 8.75 (major rotamer, 1H, d, J = 2.1 Hz), 8.81 (minor rotamer, 1H, d, J = 2.1 Hz); MS (ESI) *m/z* $[M+H]^+$ 341; Anal. Calcd for $C_{19}H_{24}N_4O_2 \cdot C_4H_6O_6 \cdot 0.3H_2O$: C, 55.70; H, 6.22; N, 11.30. Found: C, 55.67; H, 6.26; N, 11.21.

5.1.13.

***N*-Methyl-*N*-({6-[4-(morpholin-4-yl)phenyl]pyridin-2-yl}methyl)glycinamide dihydrochloride (14b)**

To a solution of **13b** (225 mg, 0.51 mmol) in MeOH (6.0 mL) was added 4 M HCl/EtOAc (2.00 mL, 8.00 mmol). After being stirred at room temperature overnight, the mixture was concentrated in vacuo. To the residue were added EtOH and EtOAc, and the resulting precipitate was filtered to give the product (199 mg, 94%) as a yellow solid. ^{1}H NMR (DMSO-d_6): this compound exists as a pair of rotamers at room temperature. δ 2.95 (minor rotamer, 3H, s), 3.12 (major rotamer, 3H, s), 3.21–3.32 (4H, m), 3.75–3.83 (4H, m), 3.96–4.06 (2H, m), 4.70 (minor rotamer, 2H, s), 4.82 (major rotamer, 2H, s), 7.09–7.20 (2H, m), 7.23–7.34 (1H, m), 7.84–8.09 (4H, m), 8.26 (3H, brs); MS (ESI) *m/z* $[M+H]^+$ 341; HRMS (ESI) *m/z* Calcted for $C_{19}H_{25}N_4O_2$ $[M+H]^+$: 341.1972, Found: 341.1975.

5.1.14. ***tert*-Butyl (2-{[3-(2-chloropyrimidin-5-yl)benzyl](methyl)amino}-2-oxoethyl)carbamate (15)**

Compound **15** was prepared from **6** and 5-bromo-2-chloropyrimidine in 79% yield as a colorless solid, using a similar approach to that described for **4a**. ^{1}H NMR ($CDCl_3$): this compound exists as a pair of rotamers at room temperature. δ 1.44 (minor rotamer, 9H,

s), 1.46 (major rotamer, 9H, s), 2.95 (major rotamer, 3H, s), 3.02 (minor rotamer, 3H, s), 3.97–4.08 (2H, m), 4.57 (minor rotamer, 2H, s), 4.68 (major rotamer, 2H, s), 5.52 (1H, brs), 7.27–7.61 (4H, m), 8.81 (major rotamer, 2H, s), 8.82 (minor rotamer, 2H, s); MS (ESI) *m/z* $[M+H]^+$ 391.

5.1.15. *tert*-Butyl {2-[(3-{2-[(2*R*)-2-(hydroxymethyl)pyrrolidin-1-yl]pyrimidin-5-yl}benzyl)(methyl)amino]-2-oxoethyl}carbamate (16a)

To a mixture of **15** (250 mg, 0.64 mmol) in DMF (5.1 mL) were added (2*R*)-pyrrolidin-2-ylmethanol (0.093 mL, 0.96 mmol) and K_2CO_3 (265 mg, 1.92 mmol). After being stirred at room temperature overnight, the mixture was diluted with water and extracted with EtOAc. The organic layer was dried over $MgSO_4$, and concentrated in vacuo. The residue was purified by column chromatography on silica gel ($CHCl_3$/MeOH = 100:0 to 95:5) to give the product (220 mg, 76%). ^{1}H NMR ($CDCl_3$): this compound exists as a pair of rotamers at room temperature. δ 1.44 (minor rotamer, 9H, s), 1.46 (major rotamer, 9H, s), 1.70–1.81 (1H, m), 1.88–2.08 (2H, m), 2.12–2.23 (1H, m), 2.92 (major rotamer, 3H, s), 3.01 (minor rotamer, 3H, s), 3.58–3.87 (4H, m), 4.02 (major rotamer, 2H, d, J = 4.3 Hz), 4.05 (minor rotamer, 2H, d, J = 4.2 Hz), 4.26–4.34 (1H, m), 4.53 (minor rotamer, 2H, s), 4.65 (major rotamer, 2H, s), 5.47–5.63 (1H, brm), 5.86 (1H, brs), 7.10–7.48 (4H, m), 8.52 (2H, s); MS (ESI) *m/z* $[M+H]^+$ 456.

5.1.16. *tert*-Butyl {2-[(3-{2-[(2*S*)-2-(hydroxymethyl)pyrrolidin-1-yl]pyrimidin-5-yl}benzyl)(methyl)amino]-2-oxoethyl}carbamate (16b)

Compound **16b** was prepared from **15** and (2*S*)-pyrrolidin-2-ylmethanol in 94% yield, using a similar approach to that described for **16a**. ^{1}H NMR ($CDCl_3$): this compound exists as a pair of rotamers at room temperature. δ 1.44 (minor rotamer, 9H, s), 1.46 (major rotamer, 9H, s), 1.71–1.81 (1H, m), 1.88–2.08 (2H, m), 2.13–2.23 (1H, m), 2.92 (major rotamer, 3H, s), 3.01 (minor rotamer, 3H, s), 3.59–3.86 (4H, m), 4.02 (major rotamer, 2H, d, J = 4.3 Hz), 4.05 (minor rotamer, 2H, d, J = 4.3 Hz), 4.26–4.35 (1H, m), 4.52 (minor rotamer, 2H, s), 4.65 (major rotamer, 2H, s), 5.48–5.61 (1H, brm), 5.85 (1H, brs), 7.10–7.48 (4H, m), 8.52 (2H, s); MS (ESI) *m/z* $[M+H]^+$ 456.

5.1.17. *tert*-Butyl [2-(methyl{3-[2-(piperidin-1-yl)pyrimidin-5-yl]benzyl}amino)-2-oxoethyl]carbamate (16c)

Compound **16c** was prepared from **15** and piperidine in 89% yield, using a similar approach to that described for **16a**. ^{1}H NMR ($CDCl_3$): this compound exists as a pair of rotamers at room temperature. δ 1.44 (minor rotamer, 9H, s), 1.47 (major rotamer, 9H, s), 1.57–1.75 (6H, m), 2.92 (major rotamer, 3H, s), 3.01 (minor rotamer, 3H, s), 3.79–3.89 (4H, m), 4.02 (major rotamer, 2H, d, J = 4.3 Hz), 4.05 (minor rotamer, 2H, d, J = 4.3 Hz), 4.52 (minor rotamer, 2H, s), 4.65 (major rotamer, 2H, s), 5.49–5.64 (1H, brm), 7.07–7.48 (4H, m), 8.51 (minor rotamer, 2H, s), 8.51 (major rotamer, 2H, s); MS (ESI) *m/z* $[M+H]^+$ 440.

5.1.18. *tert*-Butyl {2-[(3-{2-[4-(2-hydroxyethyl)piperidin-1-yl]pyrimidin-5-yl}benzyl)(methyl)amino]-2-oxoethyl}carbamate (16d)

Compound **16d** was prepared from **15** and 2-(piperidin-4-yl)ethanol in 92% yield as a pale yellow oil, using a similar approach to that described for **16a**. ^{1}H NMR ($CDCl_3$): this compound exists as a pair of rotamers at room temperature. δ 1.20–1.28 (2H, m), 1.44 (minor rotamer, 9H, s), 1.46 (major rotamer, 9H, s), 1.52–1.62 (3H, m), 1.77–1.88 (2H, m), 2.87–2.99 (2H, m), 2.92 (major rotamer, 3H, s), 3.01 (minor rotamer, 3H, s), 3.71–3.80 (2H, m), 4.02 (major rotamer, 2H, d, J = 4.3 Hz), 4.05 (minor rotamer, 2H, d, J = 4.3 Hz), 4.52 (minor rotamer, 2H, s), 4.65 (major rotamer, 2H, s), 4.75–4.85 (2H, m), 5.50–5.61 (1H, brm), 7.07–7.47 (4H, m), 8.51 (minor rotamer, 2H, s), 8.51 (major rotamer, 2H, s); MS (ESI) *m/z* $[M+H]^+$ 484.

5.1.19. Ethyl 1-{5-[3-({[*N*-(*tert*-butoxycarbonyl)glycyl](methyl)amino}methyl)phenyl]pyrimidin-2-yl}piperidine-4-carboxylate (16e)

To a mixture of **15** (400 mg, 1.02 mmol) in DMF (8.0 mL) were added ethyl piperidine-4-carboxylate (0.19 mL, 1.23 mmol) and K_2CO_3 (424 mg, 3.07 mmol). After being stirred at 60 °C overnight, the mixture was diluted with water and extracted with EtOAc. The organic layer was dried over $MgSO_4$, and concentrated in vacuo. The residue was purified by column chromatography on silica gel to give the product (492 mg, 94%). ^{1}H NMR ($CDCl_3$): this compound exists as a pair of rotamers at room temperature. δ 1.27 (3H, t, J = 7.1 Hz), 1.44 (minor rotamer, 9H, s), 1.46 (major rotamer, 9H, s), 1.68–1.81 (2H, m), 1.96–2.06 (2H, m), 2.55–2.64 (1H, m), 2.92 (major rotamer,

3H, s), 3.01 (minor rotamer, 3H, s), 3.06–3.17 (2H, m), 4.02 (major rotamer, 2H, d, J = 4.2 Hz) , 4.05 (minor rotamer, 2H, d, J = 4.1 Hz), 4.16 (2H, q, J = 7.1 Hz), 4.52 (minor rotamer, 2H, s), 4.65 (major rotamer, 2H, s), 4.66–4.74 (2H, m), 5.50–5.60 (1H, brm), 7.09–7.47 (4H, m), 8.52 (2H, s); MS (ESI) *m/z* $[M+H]^+$ 512.

5.1.20. Methyl 3-(1-{5-[3-({[*N*-(*tert*-butoxycarbonyl)glycyl](methyl)amino}methyl)phenyl]pyrimidin-2-yl}piperidin-4-yl)propanoate (16f)

Compound **16f** was prepared from **15** and methyl 3-(piperidin-4-yl)propanoate hydrochloride in 80% yield, using a similar approach to that described for **16e**. ^{1}H NMR ($CDCl_3$): this compound exists as a pair of rotamers at room temperature. δ 1.12–1.27 (2H, m), 1.44 (minor rotamer, 9H, s), 1.46 (major rotamer, 9H, s), 1.49–1.67 (3H, m), 1.75–1.84 (2H, brm), 2.34–2.42 (2H, m), 2.86–2.95 (2H, m), 2.92 (major rotamer, 3H, s), 3.01 (minor rotamer, 3H, s), 3.69 (3H, s), 4.02 (major rotamer, 2H, d, J = 4.3 Hz) , 4.05 (minor rotamer, 2H, d, J = 4.2 Hz), 4.52 (minor rotamer, 2H, s), 4.65 (major rotamer, 2H, s), 4.76–4.84 (2H, m), 5.49–5.60 (1H, brm), 7.08–7.46 (4H, m), 8.51 (2H, s); MS (ESI) *m/z* $[M+H]^+$ 526.

5.1.21. Ethyl 4-(4-{5-[3-({[*N*-(*tert*-butoxycarbonyl)glycyl](methyl)amino}methyl)phenyl]pyrimidin-2-yl}piperazin-1-yl)benzoate (16g)

Compound **16g** was prepared from **15** and ethyl 4-(piperazin-1-yl)benzoate in quantitative yield, using a similar approach to that described for **16e**. ^{1}H NMR ($CDCl_3$): this compound exists as a pair of rotamers at room temperature. δ 1.38 (3H, t, J = 7.1

Hz), 1.44 (minor rotamer, 9H, s), 1.47 (major rotamer, 9H, s), 2.93 (major rotamer, 3H, s), 3.02 (minor rotamer, 3H, s), 3.40–3.50 (4H, m), 3.97–4.10 (6H, m), 4.34 (2H, q, J = 7.1 Hz), 4.53 (minor rotamer, 2H, s), 4.66 (major rotamer, 2H, s), 5.49–5.62 (1H, brm), 6.88–6.96 (2H, m), 7.10–7.49 (4H, m), 7.92–8.00 (2H, m), 8.56 (2H, s); MS (ESI) *m/z* $[M+H]^+$ 589.

5.1.22. Ethyl 4-(4-{5-[3-({[*N*-(*tert*-butoxycarbonyl)glycyl](methyl)amino}methyl)phenyl]pyrimidin-2-yl}piperazin-1-yl)-3-chlorobenzoate (16h)

To a mixture of **15** (42.0 g, 107 mmol) in DMF (420 mL) were added ethyl 3-chloro-4-(piperazin-1-yl)benzoate (31.8 g, 118 mmol) and K_2CO_3 (29.7 g, 215 mmol). The mixture was stirred at 60 °C for 18 h, then cooled in ice, and diluted with water. The resulting precipitate was filtered and washed with water. The solid was purified by column chromatography on silica gel ($CHCl_3$/MeOH = 100:0 to 95:5), triturated with iPr$_2$O, and filtered to give the product (47.0 g, 70%) as a colorless solid. ^{1}H NMR ($CDCl_3$): this compound exists as a pair of rotamers at room temperature. δ 1.39 (3H, t, J = 7.1 Hz), 1.44 (minor rotamer, 9H, s), 1.47 (major rotamer, 9H, s), 2.93 (major rotamer, 3H, s), 3.02 (minor rotamer, 3H, s), 3.18–3.26 (4H, m), 3.98–4.11 (6H, m), 4.36 (2H, q, J = 7.1 Hz), 4.53 (minor rotamer, 2H, s), 4.66 (major rotamer, 2H, s), 5.48–5.60 (1H, brm), 7.05 (1H, d, J = 8.4 Hz), 7.10–7.48 (4H, m), 7.91 (1H, dd, J = 8.5, 2.0 Hz), 8.07 (1H, d, J = 2.0 Hz), 8.56 (2H, s); MS (ESI) *m/z* $[M+H]^+$ 623.

5.1.23.

***N*-(3-{2-[(2*R*)-2-(Hydroxymethyl)pyrrolidin-1-yl]pyrimidin-5-yl}benzyl)-*N*-methylglycinamide dihydrochloride (17a)**

Compound **17a** was prepared from **16a** in 54% yield as a pale yellow solid, using a similar approach to that described for **14b**. ^{1}H NMR (DMSO-d_6): this compound exists as a pair of rotamers at room temperature. δ 1.86–2.11 (4H, m), 2.90 (minor rotamer, 3H, s), 2.97 (major rotamer, 3H, s), 3.39 (1H, dd, J = 10.2, 7.4 Hz), 3.46–3.54 (1H, m), 3.55–3.62 (1H, m), 3.65 (1H, dd, J = 10.4, 3.7 Hz), 3.91 (minor rotamer, 2H, q, J = 5.6 Hz), 3.98 (major rotamer, 2H, q, J = 5.7 Hz), 4.13–4.21 (1H, m), 4.59 (minor rotamer, 2H, s), 4.62 (major rotamer, 2H, s), 7.20–7.25 (1H, m), 7.39–7.51 (2H, m), 7.53–7.58 (major rotamer, 1H, m), 7.58–7.63 (minor rotamer, 1H, m), 8.11–8.27 (3H, brm), 8.71 (major rotamer, 2H, s), 8.73 (minor rotamer, 2H, s); MS (ESI) *m/z* $[M+H]^+$ 356; Anal. Calcd for $C_{19}H_{25}N_5O_2 \cdot 1.9HCl \cdot 2.3H_2O$: C, 48.96; H, 6.81; N, 15.02; Cl, 14.45. Found: C, 49.26; H, 6.92; N, 14.67; Cl, 14.13.

5.1.24.

***N*-(3-{2-[(2*S*)-2-(Hydroxymethyl)pyrrolidin-1-yl]pyrimidin-5-yl}benzyl)-*N*-methylglycinamide dihydrochloride (17b)**

Compound **17b** was prepared from **16b** in 63% yield as a yellow solid, using a similar approach to that described for **14b**. ^{1}H NMR (DMSO-d_6): this compound exists as a pair of rotamers at room temperature. δ 1.87–2.11 (4H, m), 2.90 (minor rotamer, 3H, s), 2.97 (major rotamer, 3H, s), 3.39 (1H, dd, J = 10.4, 7.6 Hz), 3.46–3.53 (1H, m), 3.55–3.62 (1H, m), 3.65 (1H, dd, J = 10.4, 3.7 Hz), 3.91 (minor rotamer, 2H, q, J = 5.6 Hz), 3.98 (major rotamer, 2H, q, J = 5.7 Hz), 4.14–4.20 (1H, m), 4.59 (minor rotamer, 2H, s),

4.62 (major rotamer, 2H, s), 7.21–7.25 (1H, m), 7.40–7.51 (2H, m), 7.54–7.58 (major rotamer, 1H, m), 7.59–7.62 (minor rotamer, 1H, m), 8.11–8.24 (3H, brm), 8.71 (major rotamer, 2H, s), 8.73 (minor rotamer, 2H, s); MS (ESI) *m/z* $[M+H]^+$ 356; Anal. Calcd for $C_{19}H_{25}N_5O_2 \cdot 1.9HCl \cdot 2.7H_2O$: C, 48.21; H, 6.88; N, 14.80; Cl, 14.23. Found: C, 48.55; H, 7.02; N, 14.57; Cl, 13.95.

5.1.25. *N*-Methyl-*N*-{3-[2-(piperidin-1-yl)pyrimidin-5-yl]benzyl}glycinamide dihydrochloride (17c)

Compound **17c** was prepared from **16c** in 59% yield as a yellow solid, using a similar approach to that described for **14b**. ^{1}H NMR (DMSO-d_6): this compound exists as a pair of rotamers at room temperature. δ 1.50–1.57 (4H, m), 1.62–1.69 (2H, m), 2.90 (minor rotamer, 3H, s), 2.97 (major rotamer, 3H, s), 3.76–3.83 (4H, m), 3.91 (minor rotamer, 2H, q, J = 5.6 Hz), 3.98 (major rotamer, 2H, q, J = 5.7 Hz), 4.59 (minor rotamer, 2H, s), 4.62 (major rotamer, 2H, s), 7.19–7.23 (1H, m), 7.39–7.50 (2H, m), 7.52–7.56 (major rotamer, 1H, m), 7.58–7.61 (minor rotamer, 1H, m), 8.10–8.24 (3H, brm), 8.68 (major rotamer, 2H, s), 8.70 (minor rotamer, 2H, s); MS (ESI) *m/z* $[M+H]^+$ 340; HRMS (ESI) *m/z* Calcted for $C_{19}H_{26}N_5O$ $[M+H]^+$: 340.2132, Found: 340.2131.

5.1.26. *N*-(3-{2-[4-(2-Hydroxyethyl)piperidin-1-yl]pyrimidin-5-yl}benzyl)-*N*-methylglycinamide (2*R*, 3*R*)-tartrate (17d)

Compound **17d** was prepared from **16d** in 23% yield as a colorless solid, using a similar approach to that described for **5a**. ^{1}H NMR (DMSO-d_6): this compound exists as a pair of rotamers at room temperature. δ 1.00–1.14 (2H, m), 1.38 (2H, dt, J = 6.5, 6.5 Hz), 1.63–1.80 (3H, m), 2.87 (minor rotamer, 3H, s), 2.92 (major rotamer, 3H, s), 2.84–2.96 (2H, m), 3.47 (2H, t, J = 6.6 Hz), 3.59 (minor rotamer, 2H, s), 3.66 (major rotamer, 2H, s), 3.74 (2H, s, tartaric acid), 4.55 (minor rotamer, 2H, s), 4.59 (major rotamer, 2H, s), 4.64–4.73 (2H, m), 7.14–7.21 (1H, m), 7.37–7.48 (2H, m), 7.49–7.54 (major rotamer, 1H, m), 7.54–7.59 (minor rotamer, 1H, m), 8.66 (major rotamer, 2H, s), 8.68 (minor rotamer, 2H, s); MS (ESI) *m/z* $[M+H]^+$ 384; HRMS (ESI) *m/z* Calcted for $C_{21}H_{30}N_5O_2$ $[M+H]^+$: 384.2394, Found: 384.2396.

5.1.27.

1-[5-(3-{[Glycyl(methyl)amino]methyl}phenyl)pyrimidin-2-yl]piperidine-4-carboxylic acid dihydrochloride (17e)

To a mixture of **16e** (300 mg, 0.59 mmol) in MeOH (3.0 mL) was added 1 M NaOH aqueous solution (3.00 mL, 3.00 mmol). After being stirred at room temperature for 6 h, the mixture was neutralized with 1 M HCl aqueous solution and concentrated in vacuo. The residue was diluted with water and extracted with $CHCl_3$. The organic layer was dried over $MgSO_4$, and concentrated in vacuo to give

1-{5-[3-({[*N*-(*tert*-butoxycarbonyl)glycyl](methyl)amino}methyl)phenyl]pyrimidin-2-yl }piperidine-4-carboxylic acid. To a solution of 1-{5-[3-({[*N*-(*tert*-butoxycarbonyl)glycyl](methyl)amino}methyl)phenyl]pyrimidin-2-yl }piperidine-4-carboxylic acid in dioxane (5.0 mL) was added was added 4 M HCl/dioxane (1.5 mL, 6.0 mol). After being stirred at room temperature overnight, the mixture was concentrated in vacuo. The residue was purified by column chromatography on ODS silica gel (0.01 M HCl aqueous solution/MeCN = 9:1) to give the product (65 mg, 24%) as a pale yellow solid. ^{1}H NMR (DMSO-d_6): this compound exists as a pair of rotamers at room temperature. δ 1.42–1.57 (2H, m), 1.84–1.96 (2H, m), 2.53–2.64 (1H, m), 2.89 (minor rotamer, 3H, s), 2.97 (major rotamer, 3H, s), 3.06–3.19 (2H, m), 3.91 (minor rotamer, 2H, q, J = 5.5 Hz), 3.98 (major rotamer, 2H, q, J = 5.5 Hz), 4.50–4.65 (4H, m), 7.20–7.25 (1H, m), 7.38–7.51 (2H, m), 7.53–7.58 (major rotamer, 1H, m), 7.58–7.63 (minor rotamer, 1H, m), 8.11–8.29 (3H, brm), 8.70 (major rotamer, 2H, s), 8.73 (minor rotamer, 2H, s); MS (ESI) *m/z* $[M+H]^+$ 384; HRMS (ESI) *m/z* Calcted for $C_{20}H_{26}N_5O_3$ $[M+H]^+$: 384.2030, Found: 384.2031.

5.1.28.

3-{1-[5-(3-{[Glycyl(methyl)amino]methyl}phenyl)pyrimidin-2-yl]piperidin-4-yl}propanoic acid dihydrochloride (17f)

Compound **17f** was prepared from **16f** in 93% yield as a pale yellow solid, using a similar approach to that described for **17e**. ^{1}H NMR (DMSO-d_6): this compound exists as a pair of rotamers at room temperature. δ 0.99–1.13 (2H, m), 1.48 (2H, dt, J = 7.2, 7.2 Hz), 1.51–1.62 (1H, m), 1.68–1.79 (2H, m), 2.27 (2H, d, J = 7.5 Hz), 2.85–2.95 (2H, m), 2.89 (minor rotamer, 3H, s), 2.97 (major rotamer, 3H, s), 3.91 (minor rotamer, 2H, q, J = 5.6 Hz), 3.98 (major rotamer, 2H, q, J = 5.5 Hz), 4.59 (minor rotamer, 2H, s), 4.62 (major rotamer, 2H, s), 4.64–4.75 (2H, m), 7.19–7.25 (1H, m), 7.38–7.50 (2H, m), 7.52–7.57 (major rotamer, 1H, m), 7.57–7.62 (minor rotamer, 1H, m), 8.08–8.25 (3H, brm), 8.68 (major rotamer, 2H, s), 8.70 (minor rotamer, 2H, s); MS (ESI) *m/z* $[M+H]^+$ 412; HRMS (ESI) *m/z* Calcted for $C_{22}H_{30}N_5O_3$ $[M+H]^+$: 412.2343, Found: 412.2344.

5.1.29.

4-{4-[5-(3-{[Glycyl(methyl)amino]methyl}phenyl)pyrimidin-2-yl]piperazin-1-yl}benzoic acid dihydrochloride (17g)

Compound **17g** was prepared from **16g** in 62% yield as a colorless solid, using a similar approach to that described for **17e**. ^{1}H NMR (DMSO-d_6): this compound exists as a pair of rotamers at room temperature. δ 2.90 (minor rotamer, 3H, s), 2.97 (major rotamer, 3H, s), 3.42–3.49 (4H, m), 3.87–4.01 (6H, m), 4.60 (minor rotamer, 2H, s), 4.63 (major rotamer, 2H, s), 7.03 (2H, d, J = 9.1 Hz), 7.24 (1H, d, J = 7.6 Hz), 7.40–7.52 (2H, m),

7.55–7.60 (major rotamer, 1H, m), 7.60–7.65 (minor rotamer, 1H, m), 7.81 (2H, d, *J* = 9.0 Hz), 8.13–8.27 (3H, brm), 8.75 (major rotamer, 2H, s), 8.77 (minor rotamer, 2H, s); MS (ESI) *m/z* $[M+H]^+$ 461; HRMS (ESI) *m/z* Calcted for $C_{25}H_{29}N_6O_3$ $[M+H]^+$: 461.2296, Found: 461.2296.

5.1.30.

3-Chloro-4-{4-[5-(3-{[glycyl(methyl)amino]methyl}phenyl)pyrimidin-2-yl]piperazin-1-yl}benzoic acid dihydrochloride (17h)

To a solution of **16h** (50.6 g, 81.2 mmol) in EtOH (506 mL)/THF (506 mL) was added 1 M NaOH aqueous solution (162 mL, 162 mmol). After being stirred at room temperature overnight, the mixture was concentrated in vacuo. The residue was dissolved in H_2O (300 mL) and neutralized with 1 M HCl aqueous solution. The mixture was extracted with $CHCl_3$/MeOH (95:5). The organic layer was dried over $MgSO_4$, and concentrated in vacuo. The residue was purified by column chromatography on silica gel ($CHCl_3$/MeOH = 95:5 to 85:15) to give a solid. This solid was suspended in EtOH (500 mL) and the mixture was refluxed for 1 h. After being cooled to room temperature, the resulting precipitate was filtered to give 4-(4-{5-[3-({[*N*-(*tert*-butoxycarbonyl)glycyl](methyl)amino}methyl)phenyl]pyrimidin-2-yl}piperazin-1-yl)-3-chlorobenzoic acid (45.0 g, 93%) as a colorless solid. To a

mixture of 4-(4-{5-[3-({[*N*-(*tert*-butoxycarbonyl)glycyl](methyl)amino}methyl)phenyl]pyrimidin-2-yl}piperazin-1-yl)-3-chlorobenzoic acid (43.0 g, 72.3 mmol) in dioxane (430 mL) was added was added 4 M HCl/dioxane (253 mL, 1.01 mol). After being stirred at room temperature overnight, the resulting precipitate was filtered to give a solid. The mixture of this solid in THF/H_2O (97:3, 500 mL) was stirred at 60 °C, and then at room temperature overnight. The resulting precipitate was filtered and washed with THF to give the product (40.2 g, 98%) as a pale yellow solid. ^{1}H NMR (DMSO-d_6): this compound exists as a pair of rotamers at room temperature. δ 2.90 (minor rotamer, 3H, s), 2.98 (major rotamer, 3H, s), 3.11–3.25 (4H, m), 3.86–4.06 (6H, m), 4.61 (minor rotamer, 2H, s), 4.63 (major rotamer, 2H, s), 7.20–7.31 (2H, m), 7.40–7.53 (2H, m), 7.54–7.60 (major rotamer, 1H, m), 7.60–7.66 (minor rotamer, 1H, m), 7.86 (1H, dd, J = 8.3, 1.8 Hz), 7.91 (1H, d, J = 1.8 Hz), 8.16–8.34 (3H, brm), 8.76 (major rotamer, 2H, s), 8.78 (minor rotamer, 2H, s); MS (ESI) *m/z* $[M+H]^+$ 495; Anal. Calcd for $C_{25}H_{27}ClN_6O_3 \cdot 1.9HCl \cdot 3.6H_2O$: C, 47.73; H, 5.78; N, 13.36; Cl, 16.34. Found: C, 47.59; H, 5.67; N, 13.31; Cl, 16.20.

5.2. Molecular modeling

5.2.1. Human VAP-1 model

A side-chain conformational search and minimization for Leu469 of the three-dimensional (3D) structure of VAP-1 with TPQ in an active conformation (PDB-code: 2C11,[21] resolution: 2.90 Å) was performed using the Low Mode MD[22] function in the Molecular Operating Environment (MOE) program[18a] with an MMFF94x forcefield. The bound 2-hydrazinopyridine ligand was then deleted.

5.2.2. Docking study

The ligand molecules were prepared using LigPrep[23] and Confgen[24], and the energy-minimized conformation was used to input molecules into the follow docking calculations. Compounds were docked to the human VAP-1 model using the docking program GOLD version 5.2.[25] The ligand-binding pocket was defined using $C^{\beta}H$ from Leu468 as the central atom with a radius of 20 Å. The ligand was docked covalently to nitrogen atom N1 of PAQ1729 (PAQ is used PDB entry 2C11[21]) to assign TPQ and the ligand. Each ligand was docked 10 times.

5.2.3. Calculation of atomic charge distribution

The docking results of compound **1** and **5b** with the human VAP-1 model were used. The electrostatic potential-fitted atomic partial charges were calculated using Amber10:EHT forcefield in MOE. Analytic Connolly surfaces that surrounded the Van der Waals surfaces of the ligands or receptor were generated and colored red for negative charge and blue for positive charge using the program MOE.

5.3. Inhibitory effect on human and rat VAP-1 enzyme activity

Human and rat VAP-1 enzyme activity was measured by a radiochemistry-enzymatic assay using ^{14}C-benzylamine (American Radiolabeled Chemicals, STL, USA).[26] An enzyme suspension prepared from CHO (Chinese Hamster Ovary) cells expressing a human or rat VAP-1 enzyme was preincubated with the test compound in a 96-well microplate at room temperature for 20 min. Subsequently, the enzyme suspension was incubated with ^{14}C-benzylamine (final concentration of 1×10^{-5} mol/L) to a final volume of 50 μL at 37 °C for 1 h. The enzymatic reaction was stopped by the addition of 2 mol/L (50 μL) of citric acid. The oxidation products were extracted directly in a 200-μL toluene scintillator, and the radioactivity was measured with a scintillation spectrometer.

5.4. Inhibitory effect on CYP 3A4 and CYP2C19 activity

Each test compound (5 μM) was co-incubated with midazolam (1.5 μM), *S*-mephenytoin (30 μM), phenacetin (20 μM), amodiaquine (0.1 μM), diclofenac (10 μM), and dextromethorphan (7 μM) in a reaction medium containing 0.1 mg/mL human liver microsomes, 100 mM Na-K phosphate buffer (pH 7.4), and 1 mM NADPH at 37 °C for 20 min. At the end of the incubation, the reaction was terminated by the addition of aqueous solution containing 80% acetonitrile. The concentrations of 1'-hydroxymidazolam and 4'-hydroxymephenytoin were determined by LC-MS/MS analysis to monitor CYP3A4 and CYP2C19 activity, respectively. Inhibition of CYP3A4 and CYP2C19 activity was assessed by comparing the amount of these metabolites formed in the presence and absence of the test compound. Residual activities were calculated using the following equation.

% Residual activity = Activity compound/Activity vehicle × 100

where activity compound is activity in the presence of the test compound, and activity vehicle is activity in the absence of the test compound.

5.5. Animal experiments

All animal experimental procedures were approved by the Institutional Animal Care and Use Committee of Astellas Pharma Inc. The Tsukuba Research Center of Astellas

Pharma Inc. has been awarded Accreditation Status by the AAALAC International. All efforts were made to minimize the number of animals used and to avoid suffering and distress.

5.5.1. Inhibitory effect on plasma VAP-1 enzyme activity in rat

Male Wistar rats were purchased from Japan Charles River Laboratories (Yokohama, Japan). Blood samples for the measurement of VAP-1 activity were collected via the tail vein under diethyl ether anesthesia through a heparinized capillary. Blood was sampled before and 1 h after the oral administration of test compounds. The collected blood was placed into sampling tubes (1.5 mL), cooled in iced water and centrifuged at 4 °C to obtain plasma. The resulting plasma was stored at -80 °C until measurement of plasma VAP-1 activity.

Plasma VAP-1 activity was measured using a radioenzyme assay with a substrate of ^{14}C-benzylamine (American Radiolabeled Chemicals, STL, USA).[26] Total VAP-1 activity was measured by reacting a mixture of 100 µL rat plasma with 10 µL ^{14}C-benzylamine at 37 °C for 2 h, and non-specific activity was measured with 10 µL FR299676 (a specific VAP-1 inhibitor; Astellas Pharma Inc., 1 mmol/L) under the same conditions. Radioactivity of the reaction metabolite (^{14}C-benzaldehyde) was measured with a liquid scintillation counter (TRI-CARB 2100TR; Perkin Elmer Japan,

Yokohama, Japan). Total and non-specific VAP-1 activities (pmol) were calculated using the measured radioactivity and the radioactivity of a standard with ^{14}C-benzylamine. Plasma VAP-1 activity and inhibition ratio were calculated by the following formula:

Plasma VAP-1 activity (pmol/mL/h) = [total activity (pmol) – non-specific activity (pmol)] × [1000/100 (μL)]/2 (h).

Inhibition ratio (%) = [Plasma VAP-1 activity (before dosing) − Plasma VAP-1 activity (1 h or 6 h after dosing)]/Plasma VAP-1 activity (before dosing) × 100

5.5.2. Effect on proteinuria in STZ rat

Male Sprague Dawley (SD) rats (6 week-old) were purchased from Japan Charles River Laboratories (Yokohama, Japan). Following 1 week of adaptation, the animals were weighed and injected intraperitoneally with 65 mg/kg streptozotocin (STZ, Sigma) in citrate-buffered saline (pH 4.5). The other group underwent sham treatment with citrate-buffered saline. Three days after the STZ injection, grouping was performed based on plasma glucose (pGlu) and body weight (BW). Group compositions were as follows: (1) sham with vehicle (0.5%MC), (2) STZ with vehicle, (3) STZ with **17h** (0.1 mg/kg), (4) STZ with **17h** (0.3 mg/kg) and (5) STZ with **17h** (1 mg/kg). Oral

administration (5 mL/kg) was conducted once daily (qd) in the morning, and begun on the day after grouping and continued for 4 weeks.

Urine and blood samples were collected in the fourth week. Urine samples were collected with a metabolic cage for 24 h, and urine volume was measured with a graduated cylinder. Urinary protein was measured by Bradford's colorimetric assay (Bio-Rad Protein Assay Kit, Tokyo, Japan) using a SPECTRA max® M2. The blood sample for the measurement of plasma VAP-1 activity was collected via the suborbital plexus under diethyl ether anesthesia.

Plasma VAP-1 activity was measured using a radioenzyme assay using a substrate of ^{14}C-benzylamine (American Radiolabeled Chemicals, STL, USA).[26] Total VAP-1 activity was measured by reacting a mixture of 50 μL rat plasma with 10 μL ^{14}C-benzylamine at 37 °C for 1 h, and non-specific activity was measured with 10 μL FR299676 (a specific VAP-1 inhibitor, 1 mmol/L) under the same conditions. Radioactivity of the reaction metabolite (^{14}C-benzaldehyde) was measured with a liquid scintillation counter (TRI-CARB 2100TR, Perkin Elmer Japan, Osaka, Japan). Total and non-specific VAP-1 activities (pmol) were calculated using the measured radioactivity and the radioactivity of a standard with ^{14}C-benzylamine. Urinary protein excretion and plasma VAP-1 activity were calculated by the following formula:

Urinary protein excretion (mg/d) = urine protein (mg/mL) × urine volume (mL/d)

Plasma VAP-1 activity (pmol/mL/h) = [total activity (pmol) − non-specific activity (pmol)] × [1000/50 (μL)]/1(h)

5.5.3. Rat pharmacokinetic study

Male Wistar rats were purchased from Charles River Laboratories Japan, Inc. (Yokohama, Japan). Rats were fasted for approximately 18 h before dosing. Compound **17h** was administered to rats (n = 3) either intravenously (iv) or orally (po) at a dose of 1 mg/kg. For the iv study, test compound was prepared as a solution of 5% DMSO in water. For the po study, test compound was prepared as a solution of propylene glycol (PG) solvent/30%(w/v) 2-hydroxypropyl-β-cyclodextrin/1M HCl aqueous solution/water [3:4:1:2] (PG solvent: Tween80/HCO-40/PG = 1:2:4). Blood was collected from the vein using heparin as an anticoagulant, immediately chilled on ice, and centrifuged to obtain the plasma fraction. Test compound in plasma samples was extracted by deproteination with acetonitrile, and then analyzed by LC-MS/MS. Pharmacokinetic parameters were calculated from plasma concentrations of test compound using the non-compartmental analysis model.

Acknowledgements

The authors would like to recognize the outstanding contributions provided by Dr. Daisuke Suzuki who served as a medicinal chemist for this project. The authors thank Mr. Kyoichi Maeno and Dr. Susumu Watanuki for their valuable advice in the preparation of this manuscript and Drs. Koji Hattori and Fukushi Hirayama for their support. The authors also thank the staff of the Astellas Research Technologies Co., Ltd. for conducting elemental analysis, and spectral measurements.

References and notes

1. Gross, J. L.; de Azevedo, M. J.; Silveiro, S. P.; Canani, L. H.; Caramori, M. L.; Zelmanovitz, T. *Diabetes Care*, **2005**, *28*, 176.
2. International Diabetes Federation. IDF Diabetes Atlas 7th edition. http://www.diabetesatlas.org/
3. (a) Arora, M. K.; Singh, U. K. *Vascul. Pharmacol*. **2013**, *58*, 259; (b) Wada, J.; Makino, H. *Clin. Sci.* **2013**, *124*, 139; (c) Yamagishi, S.; Matsui, T. *Oxid. Med. Cell. Longev.* **2010**, *3*, 101; (d) Dronavalli, S.; Duka, I.; Bakris, G. L. *Nat. Clin. Pract. Endocrinol. Metab*. **2008**, *4*, 444; (e) Yu, P. H.; Wright, S.; Fan, E. H.; Lun, Z. R.;

Gubisne-Harberle, D. *Biochim. Biophys. Acta*, **2003**, *1647*, 193; (f) Hernandez, M.; Solé, M.; Boada. M.; Unzeta, M. *Biochim. Biophys. Acta*, **2006**, *1763*, 164.

4. Inzucchi, S. E.; Bergenstal, R. M.; Buse, J. B.; Diamant, M.; Ferrannini, E.; Nauck, M.; Peters, A. L.; Tsapas, A.; Wender, R.; Matthews, D. R. *Diabetes Care*, **2015**, *38*, 140.

5. (a) Boomsma, F.; van den Meiracker, A. H.; Winkel, S.; Aanstoot, H. J.; Batstra. M. R.; Man in 't Veld, A. J.; Bruining, G. J. *Diabetologia*, **1999**, *42*, 233; (b) Abella, A.; García-Vicente, S.; Viguerie. N.; Ros-Baró, A.; Camps, M.; Palacín, M.; Zorzano, A.; Marti. L. Diabetologia, **2004**, *47*, 429; (c) Boomsma, F.; Bhaggoe, U. M.; van der Houwen, A. M.; van den Meiracker, A. H., *Biochim. Biophys. Acta*, **2003**, *1647*, 48.

6. Pannecoeck, R.; Serruys, D.; Benmeridja, L.; Delanghe, J. R.; van Geel, N.; Speeckaert, R.; Speeckaert M. M. *Crit. Rev. Clin. Lab. Sci*. **2015**, *52*, 284.

7. (a) Merinen, M.; Irjala, H.; Salmi, M.; Jaakkola, I.; Hänninen, A.; Jalkanen, S. *Am. J. Pathol.* **2005**, *166*, 793; (b) Mazzone, T.; Chait, A.; Plutzky, J. *Lancet*, **2008**, *371*, 1800.

8. Buffoni, F.; Ignesti, G. *Mol. Genet. Metab*. **2000**, *71*, 559.

9. Yamaki, S.; Suzuki, D.; Fujiyasu, J.; Neya, M.; Nagashima, A.; Kondo, M.; Akabane, T.; Kadono, K.; Moritomo, A.; Yoshihara, K. *Bioorg. Med. Chem.* **2017**, *25*, 187.

10. Kumar, S.; Sharma, R.; Roychowdhury, A. *Curr. Med. Chem.* **2012**, *19*, 3605.

11. The synthesis of compound **2** was reported. See Ref. 9.

12. Connolly, M. L. *J. Appl. Cryst*. **1983**, *16*, 548.

13. Gleeson, M. P. *J. Med. Chem.* **2008**, *51*, 817.

14. ACD/Percepta, version 14.0.0, Advanced Chemistry Development, Inc., Toronto, ON, Canada, www.acdlabs.com, 2013.

15. Nakamura, T.; Kakinuma, H.; Umemiya, H.; Amada, H.; Miyata, N.; Taniguchi, K.; Bando, K.; Sato, M. *Bioorg. Med. Chem. Lett.* **2004**, *14*, 333.

16. (a) Cetina, M.; Nagl, A.; Prekupec, S.; Raić-Malić, S.; Mintas, M. *Acta Cryst.*, **2005**, *C61*, o158.; (b) Patel, U. H.; Patel, P. D.; Thakker, N., *Acta Cryst.*, **2007**, *C63*, o337.

17. Bissantz, C.; Kuhn, B.; Stahl, M. *J. Med. Chem.* **2010**, *53*, 5061.

18. (a) Molecular Operating Environment (MOE), 2010.10; Chemical Computing Group Inc., 1010 Sherbrooke St. West, Suite #910, Montreal, QC, Canada, H3A 2R7, 2010.; (b) MOE2014.0901, Chemical Computing Group Inc., 1010 Sherbrooke St. West, Suite #910, Montreal, QC, Canada, H3A 2R7, 2014.

19. Stegemann, S.; Leveiller, F.; Franchi, D.; de Jong, H.; Lindén, H. *Eur. J. Pharm. Sci.* **2007**, *31*, 249.

20. Ishikawa, M.; Hashimoto, Y. *J. Med. Chem.* **2011**, *54*, 1539.

21. Jakobsson, E.; Nilsson, J.; Ogg, D.; Kleywegt, G. J., *Acta Crystallogr., Set. D: Biol. Crystallogr.* **2005**, *61*, 1550.

22. Labute, P., *J. Chem. Inf. Model.*, **2010**, *50*, 792.

23. LigPrep, version 2.5; Schrödinger, LLC, New York, NY, 2012.

24. Confgen, version 2.3; Schrödinger, LLC, New York, NY, 2012.

25. (a) GOLD5.2, The Cambridge Crystallographic Data Centre, Cambridge, UK; (b) Jones, G.; Willett, P.; Glen, R.C., *J. Comput. Aided Mol. Des.* **1995**, *9*, 532; (c) Jones, G.; Willett, P.; Glen, R.C.; Andrew R. L.; Robin T., *J. Mol. Biol.* **1997**, *267*, 727.

26. Hayes, B. E.; Clarke, D. E. *Res. Commun. Chem. Pathol. Pharmacol.*, **1990**, *69*, 71.

Synthesis and pharmacological evaluation of glycine amide derivatives as novel Vascular Adhesion Protein-1 inhibitors without CYP3A4 and CYP2C19 inhibition

Susumu Yamaki,[*] Yuji Koga, Akira Nagashima, Mitsuhiro Kondo, Yoshiaki Shimada, Keitaro Kadono, Ayako Moritomo, and Kosei Yoshihara[†]

Graphical abstract

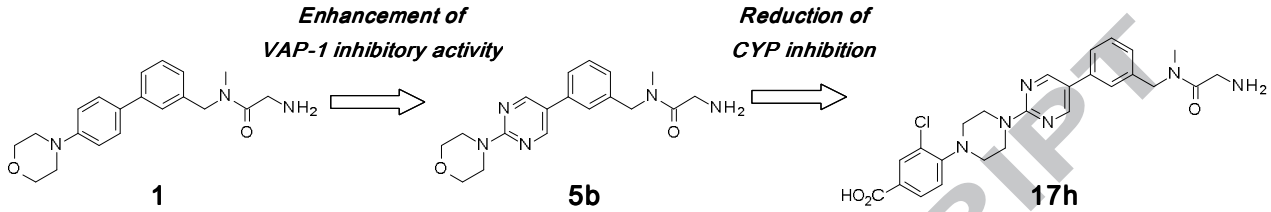

1

human VAP-1 IC_{50}: 0.34 μM

CYP inhibition (3A4, 2C19);
residual activity: 57%, 63%

5b

human VAP-1 IC_{50}: 0.031 μM

CYP inhibition (3A4, 2C19);
residual activity: 91%, 74%

17h

human VAP-1 IC_{50}: 0.025 μM

CYP inhibition (3A4, 2C19);
residual activity: 98%, 109%